IET Smart Grid

Submission for IET Smart Grid

IET Journals
The Institution of Engineering and Technology

ISSN 2515-2947
doi: 0000000000
www.ietdl.org

On Statistical Power Grid Observability under Communication Constraints (invited paper)

Minglei You[1], *Jing Jiang*[1], *Andrea M. Tonello*[2], *Tilemachos Doukoglou*[3], *Hongjian Sun*[1*]

[1] *Department of Engineering, Durham University, Durham, UK*
[2] *Institute of Networked and Embedded Systems, University of Klagenfurt, Klagenfurt, Austria*
[3] *Department of Laboratories and Technologies Testing Fixed and Mobile, OTE S.A., Athens, Greece*
* *E-mail: hongjian.sun@durham.ac.uk*

Abstract: Phasor Measurement Units (PMUs) have enabled real-time power grid monitoring and control applications, which integrate both advanced power grid and communication technologies. Communication network formed by PMUs has strict latency requirements. If PMU measurements cannot reach control centre within the latency bound, they will be invalid for calculation and may compromise the observability of the whole power grid as well as related applications. To address this issue, this paper proposes a model to account for the power grid observability under communication constraints, where effective capacity is adopted to perform a cross-layer statistical analysis in the communication system. Based on this model, three algorithms are proposed for improving power grid observability, which are observability redundancy algorithm, observability sensitivity algorithm and observability probability algorithm. These three algorithms aim at enhancing the power system observability via the optimal communication resource allocation for a given grid infrastructure. Case studies show that the proposed algorithms can improve the power system performance under constrained communication resources.

1 Introduction

Phasor Measurement Units (PMUs) can provide real-time power grid measurements via advanced power system and communication technologies, which improves the performance of power grid monitoring and control [1]. The PMUs are usually installed at selected buses in the power grid, which can provide measurements of both voltage and current phasor at that bus. At the same time, the communication modules associated to PMUs also form a communication network, which is synchronised by the Global Positioning Satellite (GPS). The phasor measurements are also transmitted via this communication network [2]. Since one PMU is capable to provide the information of each branch connected to that bus besides the bus itself, we can use a relatively smaller number of PMUs to monitor the whole power grid operation status. With the real-time information from PMUs deployed across the power grid, potential applications like real-time stability enhancement and vulnerability assessments are enabled [3]. This has stimulated various researchers to investigate the optimal PMU locations for different applications [4], such as power grid observability [5], state estimation [6], cyber security [7] and deployment costs [8].

From the aspect of power grid observability, PMUs show a great advantage over RTUs. It has been proposed that maintaining certain degrees of observability redundancy will be beneficial in case of PMU failures. To this end, several algorithms have been proposed, which are able to maintain the whole power system observable in case of one or multiple PMU failures. The primary and backup (P & B) method has been proposed in [9], which consists of two independent sets of PMUs and both of them can provide full observability of the whole power grid. In [10], a local redundancy method has been proposed, which aims at guaranteeing the redundancy from the individual bus aspect. When PMU measurements are used for real-time power grid monitor, it usually requires a stringent latency performance. If the PMU measurements are not collected at the control center within a valid latency bound, these measurements will be invalid and compromise the monitoring performance of the whole power grid. However, latency is inevitable for a practical communication system.

Compared to its wired counterpart, wireless communication technology has many advantages, such as low cost, flexibility and scalability [11]. Hence wireless communication is playing a more and more important role in supporting the communication needs of modern grid [12]. In IEEE Standard 2030.2-2015 [13], the application of wireless technology for the communication between components within transmission network and the operation control center has been identified. There have been various researches addressing the wireless communication network in supporting communication between PMUs [14][15][16][17] as well as components of SCADA system [18] [19] [20]. Yet wireless communication is broadcasting in nature, which makes propagation signal prone to the influence of physical environment. The effect of channel fading will induce communication system performance fluctuation, and then result in communication delay. However, the communication delay's influence on the power system observability performance as well as the inter-discipline study of the power system and communication system has not been well addressed, which is the major focus of this paper.

Communication latency is a link layer metric used in the Open Systems Interconnection (OSI) model. In practical systems, communication delay has many sources. Some latencies are fixed or bounded, such as system overheads. Others are time-varying and hard, if not impossible, to be bounded. One major uncertainty contributed to this time-varying latency is due to the communication channel fading effect. However, typically latency is a metric considered in link layer but not physical layer, where the latency study is further complicated when the channel has parameters that change with time. Therefore it requires sophisticated cross-layer analysis to study such problems. Another challenge is that, in most fading channel scenarios, it is not feasible to provide a deterministic bound for the communication delay, which is a consequence of communication performance fluctuation induced by channel fading [21]. To address these challenges, effective capacity (rate) theory is considered in this paper, which provides a cross-layer model to estimate the statistical delay bound under channel fading scenarios. The effective capacity theory is a powerful analytical tool and can be applied as a quality of service provisioning metric in various communication systems, such

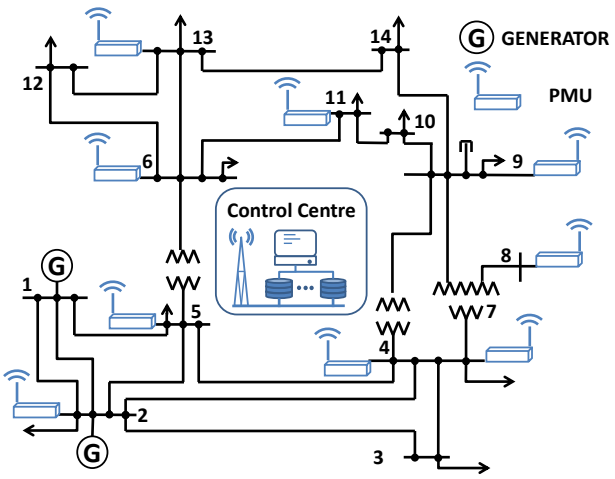

Fig. 1: IEEE 14 bus power system with 9 PMUs.

as cellular networks [22], multi-hop wireless networks [23] and cognitive radio networks [24]. Besides, in [25] [26] [27], the effective rates under various fading scenarios have been extensively studied, which makes the analysis based on effective rate readily applicable to the practical situations.

In this paper, the power system observability under communication constraints is studied. The major contributions are the following,

- We propose a model to account for the power grid's observability under constraint communication resources, which addresses the coupling effects of the power system and wireless communication system.
- The influence of wireless channel fading phenomena on the observability has been characterised using a statistical analysis and cross-layer analysis method. It provides a promising and general analysis method to bound the uncertainty effects due to wireless communication reliability.
- Three observability optimisation algorithms are proposed via an optimal communication resource allocation. The algorithms are focusing on different performance metrics of observability, which are the observability redundancy, observability sensitivity and observability probability.

The rest of this paper is structured as follows. In Section 2, the PMU based power system observability is reviewed, while the power system observability under communication constraints is studied and modelled in Section 3. The effective capacity theory is studied in Section 4, which provides a communication system cross-layer analysis framework to fill the research gap between the statistical power system observability analysis and the constraint communication resources. Then three observability improvement algorithms are proposed in Section 5, while case studies are performed in Section 6. Finally, conclusions are drawn in Section 7.

2 PMUs Based Power System Observability

With the PMU deployment, a lot of real-time applications have been enabled, such as state estimation, adaptive relaying and voltage instability enhancement. Compared to traditional measurement methods, PMUs are more versatile and they can provide more timely information about the power grid. Fig. 1 illustrates a typical IEEE 14 bus power system. When a bus is installed with a PMU and all branches are monitored, the PMU can measure the bus phasor voltage and outgoing current phasor information on the connected branches. The PMU can be also configured to monitor only some of the branches, but in this paper, it is assumed that all connected branches are monitored.

In an N bus power system, let the binary column vector $\mathbf{X} = \{x_1, x_2, \ldots, x_N\}^T$ denote the PMU installation vector, where $(\cdot)^T$ is transpose operator. Its elements are given by

$$x_i = \begin{cases} 1, & \text{if a PMU is installed at bus } i, \\ 0, & \text{otherwise.} \end{cases} \tag{1}$$

Furthermore, it is assumed that the system has installed K PMUs, which are labelled as PMU_k, where $k = 1, 2, \ldots, K$ and $K \leq N$. It can be verified that $K = \sum_{i=1}^{N} x_i$.

It is assumed that the grid topology is known as a priori for a given power grid. That is, the elements of binary network connectivity matrix $\mathbf{H}$ are known and given by [9]

$$h_{ij} = \begin{cases} 1, & \text{if bus } i \text{ and } j \text{ are connected or } i = j, \\ 0, & \text{otherwise.} \end{cases} \tag{2}$$

A bus will be observable if at least one PMU is placed at that bus or any bus incident to it [10]. Hence, the bus observability vector $\mathbf{b}$ can be given as [8]

$$\mathbf{b} = \mathbf{H}\mathbf{X}, \tag{3}$$

where each element b_i in the bus observability vector $\mathbf{b}$ indicates the number of PMUs connected to or located at bus i, we have

$$b_i = \sum_{j=1}^{N} h_{ij} x_j. \tag{4}$$

It should be noticed that the observability vector $\mathbf{b}$ in (3) and its element b_i in (4) are defined based on mathematical expectations. Hence the power grid is expected to be observable if $\mathbf{b} \geq \mathbf{1}_N$, i.e. $b_i \geq 1, \forall i$. If $b_i = 0$ for some i, the associated bus will not be expected to be observable. It can be seen that this grid observability model considers both power grid topology and PMU installation features. In the next section, an extended model will be proposed with the consideration of communication constraints.

3 Grid Observability under Communication Constraints

In this section, we will further extend the observability definition in Section 2 to account for communication constraints. For a practical power system, the system statuses, such as currents, voltages and angles, would vary with time. Hence the real-time grid status monitoring of the power grid has a stringent latency requirement. To maintain real-time performance, each measurement from the PMUs will be valid within a delay bound $D_{\max}$. If the measurement packages have been delayed longer than $D_{\max}$, then these measurements can not be used, which results in a compromised power grid status monitoring performance. The latency has many contributors, such as processing overheads and transmission delays, which are usually fixed values for a considered scenario. However, within wireless communication systems, the latency resulting from the channel fading effect usually varies with time and it is hard to bound. In ideal cases, the communication systems should be designed to provide a 100 percent guarantee that the communication delay d_k of PMU_k is smaller than $D_{\max}$. However, in practice, it has been identified that it is not feasible to provide a deterministic delay bound for the communication system in most fading channel environment [21]. Hence instead, we consider the probability $0 \leq p_k \leq 1$ to guarantee the communication delay within a certain maximum allowed bound $D_{\max}$, that is

$$\Pr\{d_k \leq D_{\max}\} \geq p_k. \tag{5}$$

Based on this, we can provide a statistical measure for the communication and the power system performance. It should be noted that in Section 5, we will show that providing 100% statistical guarantee is not cost effective. However, the power system performance under ideal communication scenarios can be approached

via a trade-off between power system and communication system performances, which will be detailed in Section 5.

Furthermore, we define the diagonal probability matrix $\mathbf{\Lambda}_P = \text{diag}\{P_1, P_2, \ldots, P_N\}$, whose elements are given by

$$P_i = \begin{cases} p_k, & \text{if PMU}_k \text{ installed at bus } i, \\ 0, & \text{otherwise.} \end{cases} \tag{6}$$

For the real-time grid monitoring, if the latency of the measurements from a certain PMU exceeds $D_{\max}$, then this information will not be used. In this paper, power grid observability vector $\bar{\mathbf{b}}$ under statistical latency guarantee can be defined as follows

$$\bar{\mathbf{b}} = \mathbf{H}\mathbf{\Lambda}_Q\mathbf{X}, \tag{7}$$

where $\mathbf{\Lambda}_Q$ denotes the diagonal communication constraint matrix, which is defined by

$$\mathbf{\Lambda}_Q = \text{diag}\{Q_1, Q_2, \ldots, Q_N\}, \tag{8}$$

where Q_i, $i = 1, 2, \ldots, N$, is a binary random variable, which can be given by

$$\begin{cases} \Pr\{Q_i = 1\} = P_i, \\ \Pr\{Q_i = 0\} = 1 - P_i. \end{cases} \tag{9}$$

Therefore, the observability vector $\bar{\mathbf{b}}$ is a vector of random variables. In this paper, we focus on the observability compromised by communication performance fluctuation, where the fluctuation is due to communication channel fading effect. PMUs are installed at selected buses, which are physically and geographically separated. Hence without loss of generality, it is assumed that random variables Q_i are independent of each other. By using the fact that $\mathbf{H}$ and $\mathbf{X}$ are known, the expected power grid observability vector $\tilde{\mathbf{b}}$ is given by

$$\tilde{\mathbf{b}} = \mathbf{H}\mathbf{\Lambda}_P\mathbf{X}. \tag{10}$$

The physical meaning of each element $\tilde{b}_i, i = 1, 2, \ldots, N$ of the expected grid observability $\tilde{\mathbf{b}}$ is that, the bus status information is available from an average of $\tilde{b}_i$ PMUs connected to the bus i. If any element $\tilde{b}_i$ is smaller than 1, then it means that the observability of this bus will not be guaranteed in a statistical view, and the power grid is vulnerable to the loss of the observability of that bus.

From the power system's aspect, a full observability of the system only requires all bus observability to be one. Any extra information about that bus can be regarded as observability redundancy to that bus. The observability redundancy is not only beneficial to cope with possible PMU failures, but also to improve the grid security [7]. In this paper, three different algorithms are proposed to improve the observability under a given grid infrastructure, which will be detailed in Section 5.

From (7) and (10), it can be proved that the power grid observability vector $\bar{\mathbf{b}}$ as well as the expected power grid observability $\tilde{\mathbf{b}}$ will be enhanced if the p_k for all PMUs are kept to be as close to 1 as possible. However, in practical systems, the communication system has a limited total bandwidth B^{th}. This can be defined as a constraint for the bandwidth B_k assigned to each PMU$_k$, that is

$$\sum_{k=1}^{K} B_k \leq B^{\text{th}}. \tag{11}$$

It can be seen that the communication constraint only confines the total available bandwidth resources to each PMU, while it is the probability p_k that is directly related to the observability. Besides, the throughput of wireless communication system is time varying due to channel fading effect. This channel fading effect on the physical layer performance will also influence the upper layers, which will result in the latencies experienced by PMUs based applications. This research gap requires a cross-layer analysis within the communication system, which will be addressed in the next section.

4 Cross Layer Statistical Delay Analysis

In communication systems, Shannon channel capacity is one of the most important performance indexes, which defines the maximum achievable rate for a given channel. According to Shannon channel capacity theorem, the capacity for a given channel is determined by channel bandwidth B and signal-to-noise ratio (SNR), which can be given as follows,

$$C = B\log_2(1 + \text{SNR}). \tag{12}$$

The variation of instant SNR will affect the instant system throughput in the physical layer, and then results in delay at the link layer. One major source for the SNR fluctuation is channel fading, which is characterized by the physical wireless communication channel. Yet the delay aspect is not considered in the formulation above. For real-time services, such as the considered PMU based system in this paper, we require a bounded delay. If a received PMU measurement packet violates its delay bound, it will not be used and this may compromise the overall performance. It is hard or infeasible to provide a deterministic delay bound, which is due to the fact that the channel fading attenuation varies with time [21]. Hence instead, we aim to provide a statistical delay bound guarantee for the power system. In this paper, effective capacity (rate) theory is adopted, which models the cross-layer relation between the link layer behaviour and the physical channel statistical characteristics [28].

Effective capacity is the dual concept of effective bandwidth [29], and it is defined as the maximum constant rate that a fading channel can support under statistical delay constraints. The effective capacity function can be written as [27]

$$R(\theta, B) = -\frac{1}{\theta T}\ln\mathbb{E}\left\{e^{-\theta TC}\right\}, \tag{13}$$

where C denotes the instantaneous Shannon channel capacity with block transmission of duration T. The parameter θ is called QoS exponent, which is a non-negative value. The minimum required QoS exponent θ_0 is the value that makes the effective capacity equal to the source rate. In order to guarantee the delay performance, the QoS exponent θ has to satisfy the constraint $\theta \geq \theta_0$. Moreover, when $\theta_0 \to 0$, the effective capacity approaches Shannon's capacity [30].

For PMU$_k$, its effective capacity can be given as

$$R_k(\theta_k, B_k) = -\frac{1}{\theta_k T}\ln\mathbb{E}_{\gamma_k}\{e^{-\theta_k T B_k \log_2(1+\rho_k\gamma_k)}\}, \tag{14}$$

where ρ_k is the average transmit SNR, which is decided by the transmit power of the communication system. The parameter γ_k is the instantaneous channel power gain, which is determined by the fading channel characteristics.

With the definition of effective capacity and applying queuing theory, the probability of d_k within $D_{\max}$ can be given by [28]

$$\Pr\{d_k \leq D_{\max}\} = 1 - e^{-\theta_k R_k(\theta_k, B_k) D_{\max}}. \tag{15}$$

In this paper, it is assumed that PMU$_k$ generates the measurements at a constant rate of R_k^{th}. The effective capacity should be no smaller than the rate R_k^{th} in order to avoid unstable status, that is

$$R_k(\theta_k, B_k) \geq R_k^{\text{th}}. \tag{16}$$

By using (14)–(16), the effective capacity theory provides a cross-layer analysis framework for the study between channel fading effect, delay bound and its associated delay bound violation probability. This probability is the same one defined in (5), which affects power system observability. Hence the communication constraints' influence on the power system observability can be characterized via the effective capacity theory. Based on this, we can provide algorithms to improve the power system performance via the optimal communication resource allocation.

In Section 5, the effective capacity theory will be exploited as an analysis tool for improving the power grid observability. To facilitate the discussions in Section 5, we first introduce the properties of effective capacity R_k here.

Lemma 1. *The effective capacity defined in* (14) *has the following properties*

$$\frac{\partial R_k(\theta_k, B_k)}{\partial B_k} \geq 0 \quad \textit{and} \quad \frac{\partial R_k(\theta_k, B_k)}{\partial \theta_k} \leq 0, \forall k \tag{17}$$

and $R_k(\theta_k, B_k)$ is concave in B_k and θ_k.

Proof: Taking the partial derivative of $R_k(\theta_k, B_k)$ in (14) with respect to B_k and using the fact that θ_k and B_k are both positive, the first term of (17) can be obtained. Then using Holder's inequality [31, eq.(1.7.5)], it can be proved that R_k is concave in B_k. Applying similar procedure, the partial derivative and convexity features of $R_k(\theta_k, B_k)$ can be obtained. Interested reader can refer to [21, 32] for more details. □

In theoretical communication system analysis, Shannon capacity defined in (12) is usually used to calculate the minimum required bandwidth, which is denoted as $B^{\text{th}}_{\text{min}}$ in this paper. For a practical system, the allocated bandwidth B^{th} has to be larger than $B^{\text{th}}_{\text{min}}$, in order to have better latency performance. If the total bandwidth is below $B^{\text{th}}_{\text{min}}$, it is for sure that the throughput of the communication system is less than the rate of the PMU measurement messages, which will lead to communication failure. Hence throughout this paper, it is assumed that $B^{\text{th}} > B^{\text{th}}_{\text{min}}$ has been enforced. Then with the properties of the effective capacity R_k, we can prove the convexity of probability p_k as follows.

Proposition 1. *The probability p_k defined in* (15) *is convex in B_k and θ_k.*

Proof: As $R_k(\theta_k, B_k)$ is concave in B_k proved in Lemma 1, $-\theta_k R_k(\theta_k, B_k) D_{\text{max}}$ is convex in B_k. Using the definition in (15), it can be proved that p_k is convex in B_k. Following the same procedure, the convexity of p_k in θ_k can be obtained. □

The probability p_k is the bridge between the observability analysis (10) and the communication constraints defined in (11). Furthermore, the convexity property of p_k will be useful in finding the optimal communication system configuration for the power system observability, as will be shown in the next section.

5 Power Grid Observability Driven Resource Allocation Algorithms

In power systems, the real-time measurements from PMUs are used to the monitoring of power grid status. Based on these measurements, real-time applications such as voltage stability enhancement and demand-side management can be therefore enabled. Hence it is very important to guarantee the observability of buses. In this section, three algorithms are proposed to optimize the power grid observability under communication constraints, which are aiming at different power system performance metrics, that are, the observability redundancy, observability sensitivity and observability probability. Throughout this paper, it is assumed that the power grid and the PMU positions are known as a priori, where the focus is placed on the optimization of the communication system to better support the services under the given configurations.

5.1 Observability Redundancy (OR) Algorithm

The grid observability is critical to applications such as grid control or planning services, therefore the loss of bus status observability can result in serious consequences. The deployment of PMUs can provide real-time power grid status, which improves the power grid observability compared to traditional methods via power flow. But the installation of PMUs will involve vast investment, which will increase the cost of the power grid operation. In fact, when a PMU is installed on a bus, it can provide information about all buses incident to this bus besides the installed bus itself [10]. By taking advantage of this feature, the PMU installation places can be selected to achieve a trade-off between cost and power grid observability [9]. With power grid topology as a priori, it is not necessary to have PMUs installed at every bus, while the desired degree of observability redundancy can be still obtained. The observability redundancy r is considered in this paper, which is defined as follows [33],

$$r = \mathbf{1}_N^T(\tilde{\mathbf{b}} - \mathbf{1}_N) \equiv \mathbf{1}_N^T \mathbf{H} \mathbf{\Lambda}_P \mathbf{X} - N. \tag{18}$$

The metric r gives an evaluation of the overall power network observability redundancy. For a power grid with PMU installation places as a priori, the metric r is upper bounded by the ideal communication case. For a compromised communication system under resource constraints, a larger value of r means that more PMUs are expected to be available to provide measurements from a statistical view. In this part, we focus on the problem of increasing observability redundancy under communication constraints, which can be formulated as follows using the effective capacity theory,

$$\begin{aligned}
\max_{B_k, \theta_k} \quad & \mathbf{1}_N^T \mathbf{H} \mathbf{\Lambda}_P \mathbf{X} \\
\text{s.t.} \quad & R_k(\theta_k, B_k) \geq R_k^{\text{th}}, k = 1, 2, \ldots, K, \\
& p_k = 1 - e^{-\theta_k R_k(\theta_k, B_k) D_{\text{max}}}, k = 1, 2, \ldots, K, \\
& R_k(\theta_k, B_k) = -\frac{1}{\theta_k T} \ln \mathbb{E}_{\gamma_k} \{ e^{-\theta_k T B_k \log_2(1+\rho_k \gamma_k)} \}, \\
& \sum_{k=1}^{K} B_k \leq B^{\text{th}},
\end{aligned} \tag{19}$$

where (19) is simplified due to the fact that the power grid bus number N is constant. The optimal observability redundancy is always achievable with valid B^{th}, which can be given using the following proposition.

Proposition 2. *The power grid observability redundancy r defined in* (18) *is convex in $\mathbf{B} = \{B_1, \ldots, B_K\}^T$ and $\boldsymbol{\theta} = \{\theta_1, \ldots, \theta_K\}^T$, and a feasible solution to the problem* (19) *always exists with every $B^{th} > B^{th}_{min}$.*

Proof: We have the summation form of (19) as $\sum_{i=1}^{N} \sum_{k=1}^{K} h_{ik} p_k$. The convexity of the redundancy r and the constraints in (19) follows Lemma 1 and the convexity of p_k proved in Proposition 1. The solution existence follows the fact that the domain formed by all possible $\mathbf{B}$ is compact. □

Since the problem (19) is convex, the solution can be obtained via numerical methods such as Interior Point approach to obtain the optimal solutions. The Observability Redundancy (OR) algorithm has been summarised as follows.

It can be seen that the effective capacity theory bridges not only the cross-layer analysis of the communication system, but also the theoretical analysis of the power system jointly with the communication system. This cross-layer and cross-system model enables the performance optimization of both systems, as illustrated in (19).

5.2 Observability Sensitivity (OS) Algorithm

The bus with the least expected observability within the whole grid is most vulnerable to unobservability. Hence the least bus observability can reflect the power grid's sensitivity to lose bus observability. In this paper, we define the observability sensitivity as $\min_i \tilde{b}_i$, that is the least observability among all buses.

Algorithm 1: Observability Redundancy (OR) Algorithm

Initialization:

1: obtain network connectivity matrix $\mathbf{H}$, PMU installation vector $\mathbf{X}$, total bandwidths B^{th}, minimum constant rate R_k^{th}, average transmit SNR ρ_k.

2: obtain the effective rate model $R_k(\theta_k, B_k)$ according to the fading scenario.

3: initialize bandwidth B_k and QoS exponent θ_k satisfying the constraints (19).

4: initialize $n = 0$ and calculate the equivalent optimisation objective $g_n = \mathbf{1}_N^T \mathbf{H} \mathbf{\Lambda}_P \mathbf{X}$.

Repeat:

1: $n = n + 1$

2: update B_k and θ_k using Interior Point algorithm and calculate the constraint errors $\mathbf{e}_c$.

3: calculate $p_k, k = 1, \ldots, K$ and update $\mathbf{\Lambda}_P$.

4: calculate $g_n = \mathbf{1}_N^T \mathbf{H} \mathbf{\Lambda}_P \mathbf{X}$.

Until: $g_n - g_{n-1} \leq \epsilon_g$ **and** $\mathbf{e}_c \leq \boldsymbol{\epsilon}_c$.

Table 1 PMU configuration

Case	PMU Number	Bus Index
IEEE 14 bus	9	2,4,5,6,7,8,9,11,13
IEEE 30 bus	21	1,3,5,7,8–13,15,17–19,22,24–29

It can be seen that, the buses with small observability values can be viewed as the bottlenecks to the whole power grid's observability. From a statistical view, these buses have more influence on the whole power grid's observability. Therefore, the power grid observability can be improved by maximizing $\min_i \tilde{b}_i$ as follows,

$$\begin{aligned} \max_{B_k, \theta_k} \quad & \min_i \tilde{b}_i \\ \text{s.t.} \quad & R_k(\theta_k, B_k) \geq R_k^{\text{th}}, k = 1, 2, \ldots, K, \\ & p_k = 1 - e^{-\theta_k R_k(\theta_k, B_k) D_{\max}}, k = 1, 2, \ldots, K, \\ & R_k(\theta_k, B_k) = -\frac{1}{\theta_k T} \ln \mathbb{E}_{\gamma_k} \{ e^{-\theta_k T B_k \log_2(1+\rho_k \gamma_k)} \}, \\ & \sum_{k=1}^{K} B_k \leq B^{\text{th}}. \end{aligned} \tag{20}$$

Besides, it can be shown that, the maximization of the power grid observability according to the strategy above is feasible, as stated by the following proposition.

Proposition 3. *A feasible solution to the observability sensitivity algorithm defined in* (20) *always exists with every* $B^{th} > B^{th}_{min}$.

Proof: Using (10), the observability sensitivity of each bus i can be given by $\tilde{b}_i = \sum_{k=1}^{K} h_{ik} p_k$. Thus the convexity of $\tilde{b}_i$ follows the convexity of p_k in Proposition 1. Then the solution existence can be given by the minimax theorem [34]. □

The Observability Sensitivity (OS) algorithm can follow a similar procedure as the OR algorithm, where g_n is replaced with the optimisation objective given in (20). We see that the value of $\min_i \tilde{b}_i$ can also reflect the power grid's reliability to the observability loss of individual buses. With a larger value of $\min_i \tilde{b}_i$, the power grid is less sensitive to the compromised observability, which improves the power system's reliability, at least from the viewpoint of observability.

5.3 Observability Probability (OP) Algorithm

The whole power grid's observability depends on individual bus's observability. Hence besides considering the expected observability based algorithms proposed in Section 5.1 and 5.2, another algorithm is proposed in this part to provide a desired probability for the observability of individual buses above a threshold. This problem can be formulated by the optimization of the probability that each bus's observability is above a desired level as follows,

$$\begin{aligned} \max_{B_k, \theta_k} \quad & \Pr\{\bar{\mathbf{b}} \geq \boldsymbol{\lambda}\} \\ \text{s.t.} \quad & R_k(\theta_k, B_k) \geq R_k^{\text{th}}, k = 1, 2, \ldots, K, \\ & p_k = 1 - e^{-\theta_k R_k(\theta_k, B_k) D_{\max}}, k = 1, 2, \ldots, K, \\ & R_k(\theta_k, B_k) = -\frac{1}{\theta_k T} \ln \mathbb{E}_{\gamma_k} \{ e^{-\theta_k T B_k \log_2(1+\rho_k \gamma_k)} \}, \\ & \sum_{k=1}^{K} B_k \leq B^{\text{th}}. \end{aligned} \tag{21}$$

The physical meaning of the desired observability level vector $\boldsymbol{\lambda}$ can be given as follows. For the case when $\boldsymbol{\lambda} = \mathbf{1}_N$, the problem defined in (21) reduces to a statistical guarantee that every bus has unity observability. For more general cases where $\boldsymbol{\lambda} \geq \mathbf{1}_N$ and $\boldsymbol{\lambda} \neq \mathbf{1}_N$, the algorithm defined in (21) provides a desired statistical observability level for individual buses. It should be noted that $\boldsymbol{\lambda}$ is upper bounded by $\boldsymbol{\lambda}_{\max}$, which can be calculated under an ideal communication assumption.

Here we define the solution to the problem of $\bar{\mathbf{b}} \geq \boldsymbol{\lambda}$ by the diagonal matrix $\boldsymbol{\alpha}_m$, and all the solutions form a set $\{\boldsymbol{\alpha}_m\}$, where $m = 1, 2, \ldots, M$. Then we can further simplify the problem defined in (21) as follows,

$$\Pr\{\bar{\mathbf{b}} \geq \boldsymbol{\lambda}\} \equiv \Pr\{\mathbf{H} \mathbf{\Lambda}_Q \mathbf{X} \geq \boldsymbol{\lambda}\} = \sum_{m=1}^{M} \Pr\{\mathbf{\Lambda}_Q = \boldsymbol{\alpha}_m\}. \tag{22}$$

Similar to the OR algorithm discussed in Section 5.1, the optimal communication resource allocation for the maximization of the observability probability is feasible, which can be given by the following proposition.

Proposition 4. *The power gird observability probability defined in* (21) *is convex in* $\mathbf{B}$ *and* $\boldsymbol{\theta}$*, and a feasible solution always exists with* $\boldsymbol{\lambda} \leq \boldsymbol{\lambda}_{max}$ *and* $B^{th} > B^{th}_{min}$.

Proof: The desired results can be obtained following similar arguments in Proposition 2. □

The Observability Probability (OP) algorithm can follow a similar procedure as the OR algorithm, where g_n is replaced with the optimisation objective given in (21). Note that each solution $\boldsymbol{\alpha}_m$ consists of only binary elements, namely 0 and 1. Hence when the PMU installation buses are known as a priori, the solution set $\{\boldsymbol{\alpha}_m\}$ is readily available. Besides, if the measurements for some buses are critical information or critical to the whole power grid's observability, we impose such buses to offer higher desired observability levels, which can be achieved by assigning corresponding elements in the parameter $\boldsymbol{\lambda}$.

It can be seen that the application of statistical analysis is a promising way to bound the uncertainties due to communication performance variations, especially when power systems and communication systems are deeply coupled with each other. Thus the methods used in the proposed algorithms are also valuable to the research of similar problems such as PMU based grid monitoring [14][15][16][17], SCADA systems [18] [19] [20] and smart meter aggregations [35][36].

6 Case Studies

In this section, the three proposed algorithms in Section 5, i.e. the Observability Redundancy (OR) algorithm, Observability Sensitivity (OS) algorithm, Observability Probability (OP) algorithm, are verified using two case studies, namely IEEE 14 bus power system test case and IEEE 30 bus power system test case. These two test cases have been extensively used as standard test cases to verify power system performances [6] [10].

Here we apply the primary and backup (P&B) method [9] for the PMU installation. The objective of P&B method is to provide the power grid with two independent PMU sets. Either primary and backup set is capable to provide a full observability of the whole power grid. This provides the power grid with redundancy, where the whole grid is still expected to be observable when multiple PMUs fail within only one set. Without loss of generality, it is assumed that all PMUs generate measurement packages at the rate of 60kbps and the maximum allowed latency bound for these measurement packages is set to be 10ms [37] [38]. Please note that the main topic of this paper is to improve the observability from the communication aspect, where the PMU placement is assumed as a priori knowledge which only determines the upper bound for the best observability.

Moreover, it is assumed that the control centre locates at the power grid centre. The average SNR ρ_k for PMU_k is relate to the distances between control centre and the PMU, which are in the range of 10–15dB in IEEE 14 bus case and 7–12dB in IEEE 30 bus case. It is assumed that all PMU transceivers use unit transmit power. Rayleigh fading is considered as the channel fading effect for each communication channel. Under such conditions, the effective capacity under Rayleigh fading channels can be given by [27]

$$R_k(\theta_k, B_k) = -\frac{1}{\theta_k T} \ln {}_2F_0[\frac{\theta_k B_k T}{\ln 2}, 1, -\rho_k], \qquad (23)$$

where ${}_2F_0[\cdot]$ is the generalized hypergeometric function [31].

In case of PMU communication system failure, a redundancy bandwidth is always allocated to that PMU transceiver. We adopt the bandwidth allocation algorithm similar to [39] as default algorithm, where required bandwidth for the PMUs is calculated using Shannon capacity (12) and the extra bandwidth will be evenly divided and allocated to each PMU. In our proposed algorithms, the total bandwidth is allocated according to the optimal solution of (19), (20) and (21). For the OP algorithm, the desired statistical observability level is assumed to be $\boldsymbol{\lambda} = \mathbf{1}_N$. Since the problems are nonlinear optimization problems, the Interior Point approach is applied to find the optimal bandwidth allocation solution.

6.1 IEEE 14 Bus Case Study

In this part, the case of IEEE 14 bus power system has been considered, whose bus topology and PMU installation position have been shown in Fig. 1. The statistical probability of the communication delay associated to PMU at bus 2 has been given in Fig. 2. The Shannon capacity required for the PMU at bus 2 is 17.344kHz under the considered scenario. It can be indicated from Fig. 2 that the latency bound will not be met with only minimum required bandwidth. In order to counteract the fading induced communication system fluctuation, extra bandwidths are needed for a desired performance, whose quantity can be obtained via (15) and (23).

The observability redundancy under different total communication bandwidth constraints is illustrated in Fig. 3a. Here we consider the PMU loss only results from the maximum latency bound violation. Without any PMU loss, using the PMU installation position defined in Table 1, the overall grid observability redundancy can be calculated to be 25. It can be seen from Fig. 3a that the OR algorithm provides the best grid observability redundancy performance across different bandwidths. Specifically, with a total bandwidth of 163kHz, the proposed OR algorithm can provide a close performance to the situation of no PMU loss, while the default algorithm requires 169kHz to reach a similar performance.

In an ideal communication scenario, the observability sensitivity for the considered case is 2, which is due to the two independent sets

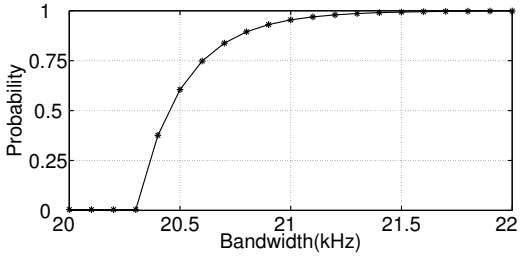

Fig. 2: The probability of communication delay bound being met associated to PMU at bus 2 as a function of bandwidth.

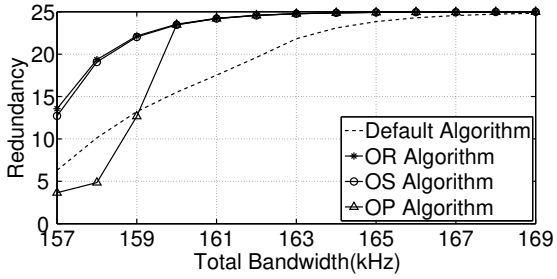

(a) Observability redundancy performance in IEEE 14 bus case.

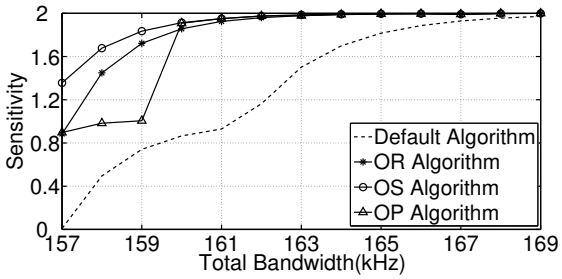

(b) Observability sensitivity performance in IEEE 14 bus case.

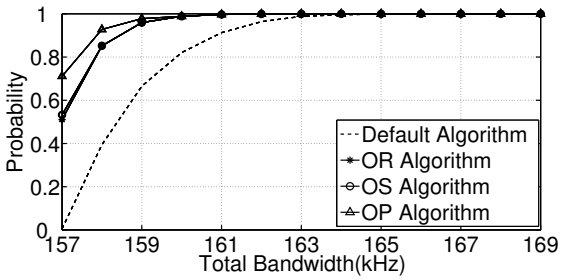

(c) Observability probability performance in IEEE 14 bus case.

Fig. 3: Power grid observability under IEEE 14 bus power system test case.

of PMUs in the P&B method. Fig. 3b indicates that the OS algorithm is capable to improve the minimum bus observability within the whole power grid. It also suggests that the OR algorithm and OS algorithm have better performance over the OP algorithm, when considering redundancy and sensitivity metrics. One major reason is that these two algorithms are both based on expected observability while the OP algorithm focuses on the probability performance.

The OP algorithm aims at improving the probability that individual bus observability is over the desired threshold. In this case study, the desired threshold has been set to be 1, which equals the case that the whole power system has unity observability. It is shown in Fig. 3c that the OP algorithm provides better statistical guarantee individual bus's observability to be larger than 1. It can be also noticed that,

this performance gain is at the cost of a reduced overall observability redundancy and observability sensitivity, as shown in Fig. 3a – 3b.

More detailed performances related to individual buses are given in Table 2 and Table 3, where the total available bandwidth is 159kHz. It is worth mentioning that, under the considered scenario, the minimum required total channel bandwidth is calculated to be 131.87kHz using Shannon capacity theorem. But it can be inferred from Table 2 that, with only Shannon capacity, the system observability cannot meet the requirement. Using default algorithm, which provides each PMU with required Shannon bandwidth and evenly divides the extra bandwidth, the bus 8 is vulnerable to losing observability in the considered scenario. On the contrary, every bus observability can be statistically guaranteed by the OR algorithm, OS algorithm or OP algorithm, where the performance has been optimized for different desired performance metrics, respectively. From Table 2 as well as Fig.3a – 3c, it can be seen that the proposed algorithms make better use of the extra bandwidth, to obtain performance improvements on observability redundancy, observability sensitivity and observability probability, respectively.

6.2 IEEE 30 Bus Case Study

In order to test the performance of the proposed algorithms, the IEEE 30 bus power system test case has also been investigated. The bus topology for the IEEE 30 bus power system is given in Fig. 4.

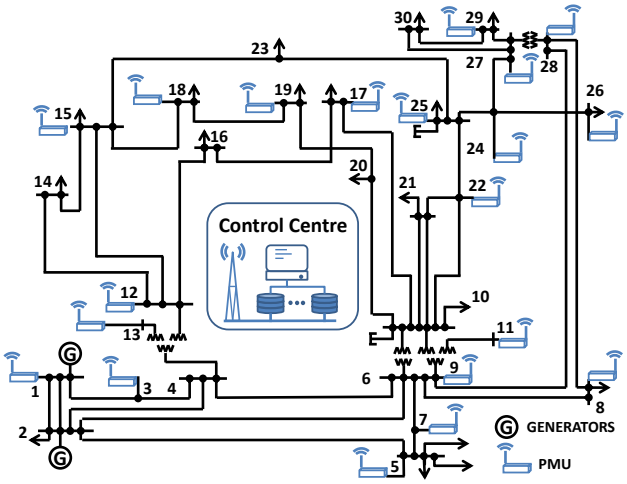

Fig. 4: IEEE 30 bus power system with 21 PMUs.

The proposed three algorithms are oriented in the optimization of three different power system performance metrics, namely observability redundancy, observability sensitivity and observability probability. The simulation results have been given in Fig. 5a–5c. It can be seen from these figures that, the three proposed algorithms have better performance overall considered performance metrics than the default algorithm in the considered scenarios.

As illustrated in Fig. 5a, the OR algorithm provides more redundancy than the OP algorithm as well as the default algorithm. From the aspect of observability redundancy, the performance gain for OR algorithm is slightly higher than OS algorithm. But this loss of performance gain in the OS algorithm improves the power grid observability sensitivity, as indicated in Fig. 5b. This is because the overall resources are constrained, which results in the situation that, the improvement of certain bus observability will be at the cost of other bus observability. Although this redundancy performance gain does not seem to be large between the OR algorithm and the OP algorithm, it should be noticed that the redundancy performance in Fig. 5a targets the whole power system performance, while the sensitivity performance in Fig. 5b targets individual buses. With constrained total resources, the improvement of overall grid observability redundancy will be less seemingly prominent in the figures

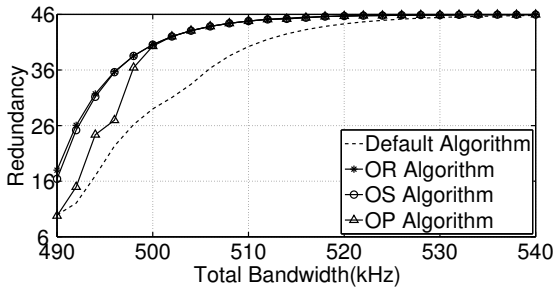

(a) Observability redundancy performance in IEEE 30 bus case.

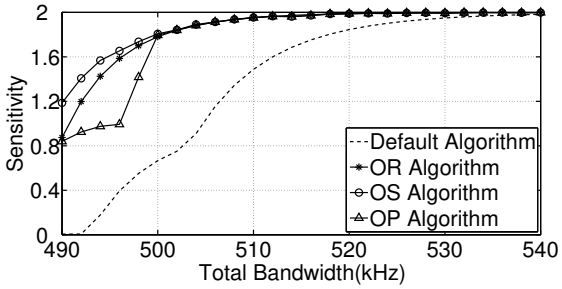

(b) Observability sensitivity performance in IEEE 30 bus case.

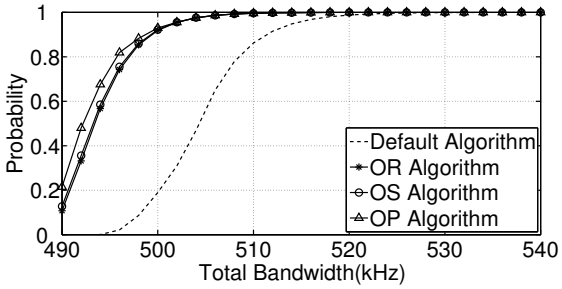

(c) Observability probability performance in IEEE 30 bus case.

Fig. 5: Power grid observability under IEEE 30 bus power system test case.

than the sensitivity performance. However, it should be noted that individual bus performances are different, as shown in Table 2 – 3.

As can be seen in Fig. 5c, the OP algorithm improves the probability that the requirement of power system observability is met over different total communication bandwidths. It can be also seen that the performance gain is at the cost of a decrease in redundancy and sensitivity performances, as can be indicated from Fig. 5a – 5b.

Comparing performances between IEEE 14 bus case in Fig. 3a – Fig. 3c and IEEE 30 bus case in Fig. 5a – Fig. 5c, the three proposed algorithms provide better observability than the default algorithm, when corresponding optimized metrics are considered. But it also indicates that no single algorithm outperforms the other algorithms if all metrics are considered at the same time. The optimal algorithm depends on the considered scenario and the metric of interest.

The considered performance metrics, namely observability redundancy, observability sensitivity and observability probability, are all formulated using a statistical approach. In theory, the best performance where an ideal communication system is considered, can be asymptotically approached. Yet from the discussion above, to improve the average performance, it has to increase the overall communication resources in an exponential way. The performance gain may be marginal even with large deployment of communication resources, especially when it is close to the best performance. Hence the results also suggest that there is a trade-off between the observability and the bandwidth. In the considered IEEE 30 bus case, the power system can reach performance similar to that with ideal communication using a total bandwidth of 520 kHz.

Table 2 Average Bus observability with a total of 159kHz bandwidth.

	Average Bus Observability														Red.	Sen.	Pr.
	1	2	3	4	5	6	7	8	9	10	11	12	13	14			
Default	1.004	1.740	0.741	3.639	2.740	3.296	2.639	0.912	2.635	1.988	1.997	1.299	1.299	1.290	13.217	0.741	0.665
OR	1.867	2.809	1.851	4.676	3.763	3.767	3.609	1.722	2.809	1.865	1.873	1.860	1.860	1.852	22.151	1.722	0.959
OS	1.844	2.774	1.835	4.657	3.715	3.669	3.706	1.835	2.813	1.835	1.835	1.835	1.835	1.835	22.023	1.835	0.959
OP	1.693	2.315	1.606	4.303	3.311	1.725	2.846	1.229	2.610	1.006	1.006	1.006	1.006	1.006	12.667	1.006	0.978

Table 3 Probability of delay within maximum allowed latency bound with a total of 159kHz bandwidth.

PMU bus location	2	4	5	6	7	8	9	11	13
Default	0.004	0.737	0.999	0.999	0.908	0.004	0.991	0.997	0.299
OR	0.909	0.942	0.958	0.954	0.921	0.801	0.946	0.919	0.906
OS	0.905	0.930	0.939	0.941	0.942	0.894	0.941	0.894	0.894
OP	0.904	0.928	0.943	0.944	0.941	0.891	0.940	0.900	0.892

7 Conclusion

In this paper, the power grid observability has been studied by jointly considering both power system and communication system. A corresponding analysis model has also been formulated. In order to perform the communication system cross-layer analysis, as well as to consider the channel fading effect and total bandwidth constraint, the effective capacity theory has been adopted and utilized. Based on this cross scenario and cross-layer analysis model, three observability metrics have been formulated, namely observability redundancy, observability sensitivity and observability probability. Then, corresponding improvement algorithms have been proposed via optimal communication resource allocation. The IEEE 14 bus and 30 bus power systems have been used in the case study to validate the performance of the three proposed algorithms. Results show that the proposed algorithms can help improve the power grid observability. Furthermore, the three proposed algorithms have the potential to be used for a trade-off between the investment needed for the communication system and the required power system performance.

8 References

1 T. Routtenberg, R. Concepcion, and L. Tong, "PMU-based detection of voltage imbalances with tolerance constraints," *IEEE Trans. Power Del.*, vol. 32, no. 1, pp. 484–494, Feb. 2017.

2 K. G. Khajeh, E. Bashar, A. M. Rad, and G. B. Gharehpetian, "Integrated model considering effects of zero injection buses and conventional measurements on optimal PMU placement," *IEEE Trans. Smart Grid*, vol. 8, no. 2, pp. 1006–1013, Mar. 2017.

3 A. G. Phadke and J. S. Thorp, *Synchronized phasor measurements and their applications*. Springer, 2008, vol. 1.

4 V. Madani, M. Parashar, J. Giri, S. Durbha, F. Rahmatian, D. Day, M. Adamiak, and G. Sheble, "PMU placement considerationsąła roadmap for optimal PMU placement," in *2011 IEEE/PES PSCE*, 2011, pp. 1–7.

5 S. Azizi, A. S. Dobakhshari, S. A. N. Sarmadi, and A. M. Ranjbar, "Optimal PMU placement by an equivalent linear formulation for exhaustive search," *IEEE Trans. Smart Grid*, vol. 3, no. 1, pp. 174–182, Feb. 2012.

6 V. Kekatos, G. B. Giannakis, and B. Wollenberg, "Optimal placement of phasor measurement units via convex relaxation," *IEEE Trans. Power Syst.*, vol. 27, no. 3, pp. 1521–1530, Feb. 2012.

7 Q. Yang and et al., "On optimal PMU placement-based defense against data integrity attacks in smart grid," *IEEE Trans. Inf. Forensics Security*, vol. 12, no. 7, pp. 1735–1750, Mar. 2017.

8 M. B. Mohammadi, R.-A. Hooshmand, and F. H. Fesharaki, "A new approach for optimal placement of PMUs and their required communication infrastructure in order to minimize the cost of the WAMS," *IEEE Trans. Smart Grid*, vol. 7, no. 1, pp. 84–93, Mar. 2016.

9 X. Bei, Y. J. Yoon, and A. Abur, "Optimal placement and utilization of phasor measurements for state estimation," *PSERC Publication*, pp. 05–20, 2005.

10 N. H. Abbasy and H. M. Ismail, "A unified approach for the optimal PMU location for power system state estimation," *IEEE Trans. Power Syst.*, vol. 24, no. 2, pp. 806–813, May 2009.

11 V. C. Gungor, D. Sahin, T. Kocak, S. Ergut, C. Buccella, C. Cecati, and G. P. Hancke, "Smart grid technologies: Communication technologies and standards," *IEEE Trans. Ind. Informat.*, vol. 7, no. 4, pp. 529–539, Feb. 2011.

12 B. A. Akyol, H. Kirkham, S. L. Clements, and M. D. Hadley, "A survey of wireless communications for the electric power system," Pacific Northwest National Laboratory (PNNL), Richland, WA (US), Tech. Rep., 2010.

13 "IEEE guide for the interoperability of energy storage systems integrated with the electric power infrastructure," *IEEE Std 2030.2-2015*, pp. 1–138, June 2015.

14 H. Gharavi and B. Hu, "Scalable synchrophasors communication network design and implementation for real-time distributed generation grid," *IEEE Trans. Smart Grid*, vol. 6, no. 5, pp. 2539–2550, Sept 2015.

15 D. Ghosh, T. Ghose, and D. K. Mohanta, "Communication feasibility analysis for smart grid with phasor measurement units," *IEEE Trans. Ind. Informat.*, vol. 9, no. 3, pp. 1486–1496, Aug 2013.

16 P. Castello, P. Ferrari, A. Flammini, C. Muscas, P. A. Pegoraro, and S. Rinaldi, "A distributed pmu for electrical substations with wireless redundant process bus," *IEEE Trans. Instrum. Meas.*, vol. 64, no. 5, pp. 1149–1157, May 2015.

17 A. Kudeshia, V. Gupta, N. Valecha, and A. K. Jagannatham, "Total variation measurement decoding (tvmd) for reliable wireless transmission of pmu measurements in smart grids," in *2017 IEEE 85th VTC Spring*, June 2017, pp. 1–5.

18 M. B. Mollah, M. A. Ullah, M. Y. Mozumder, and S. S. Islam, "Concept design for SCADA system using cognitive radio based IEEE 802.22 for power system," in *2012 IEEE CYBER*, May 2012, pp. 109–114.

19 M. B. Mollah and S. S. Islam, "Towards IEEE 802.22 based SCADA system for future distributed system," in *2012ICIEV*, May 2012, pp. 1075–1080.

20 X. Zhang, Y. Gao, G. Zhang, and G. Bi, "CDMA2000 cellular network based SCADA system," in *Proceedings. International Conference on Power System Technology*, vol. 2, 2002, pp. 1301–1306 vol.2.

21 J. Tang and X. Zhang, "Cross-layer modeling for quality of service guarantees over wireless links," *IEEE Trans. Wireless Commun.*, vol. 6, no. 12, pp. 4504–4512, Dec. 2007.

22 S. Agarwal, S. De, S. Kumar, and H. Gupta, "QoS-aware downlink cooperation for cell-edge and handoff users," *IEEE Trans. Veh. Technol.*, vol. 64, no. 6, pp. 2512–2527, Jun. 2015.

23 D. Qiao, M. Gursoy, and S. Velipasalar, "Effective capacity of two-hop wireless communication systems," *IEEE Trans. Inf. Theory*, vol. 59, no. 2, pp. 873–885, Feb. 2013.

24 Y. Yang, S. Aissa, and K. Salama, "Spectrum band selection in delay-QoS constrained cognitive radio networks," *IEEE Trans. Veh. Technol.*, vol. 64, no. 7, pp. 2925–2937, Jul. 2015.

25 M. Matthaiou, G. C. Alexandropoulos, H. Q. Ngo, and E. G. Larsson, "Analytic framework for the effective rate of MISO fading channels," *IEEE Trans. Commun.*, vol. 60, no. 6, pp. 1741–1751, Jun. 2012.

26 X. Li, J. Li, L. Li, J. Jin, J. Zhang, and D. Zhang, "Effective rate of MISO systems over κ - μ shadowed fading channels," *IEEE Access*, vol. 5, pp. 10 605–10 611, Jun. 2017.

27 M. You, H. Sun, J. Jiang, and J. Zhang, "Unified framework for the effective rate analysis of wireless communication systems over MISO fading channels," *IEEE Trans. Commun.*, vol. 65, no. 4, pp. 1775–1785, Apr. 2017.

28 D. Wu and R. Negi, "Effective capacity: a wireless link model for support of quality of service," *IEEE Trans. Wireless Commun.*, vol. 2, no. 4, pp. 630–643, Jul. 2003.

29 C.-S. Chang and J. A. Thomas, "Effective bandwidth in high-speed digital networks," *IEEE Journal on Selected Areas in Communications*, vol. 13, no. 6, pp. 1091–1100, Aug. 1995.

30 M. C. Gursoy, "MIMO wireless communications under statistical queueing constraints," *IEEE Trans. Inf. Theory*, vol. 57, no. 9, pp. 5897–5917, Sep. 2011.

31 F. W. Olver, D. W. Lozier, R. F. Boisvert, and C. W. Clark, *NIST handbook of mathematical functions*. Washington, DC: Cambridge University Press, 2010.

32 A. A. Khalek, C. Caramanis, and R. W. Heath, "Delay-constrained video transmission: Quality-driven resource allocation and scheduling," *IEEE Journal of Selected Topics in Signal Processing*, vol. 9, no. 1, pp. 60–75, Feb. 2015.

33 M. You, Q. Liu, J. Jiang, and H. Sun, "Power grid observability redundancy analysis under communication constraints." in *2017 6th IEEE/CIC ICCC*. IEEE, Oct. 2017, pp. 1–5.

34 D. Bertsekas, A. Nedić, and A. Ozdaglar, *Convex Analysis and Optimization*, ser. Athena Scientific optimization and computation series. Athena Scientific, 2003.

35 Y. Hong, W. M. Liu, and L. Wang, "Privacy preserving smart meter streaming against information leakage of appliance status," *IEEE Trans. Inf. Forensics Security*, vol. 12, no. 9, pp. 2227–2241, Sep. 2017.

36 J. Ni, K. Zhang, K. Alharbi, X. Lin, N. Zhang, and X. S. Shen, "Differentially private smart metering with fault tolerance and range-based filtering," *IEEE Trans. Smart Grid*, vol. 8, no. 5, pp. 2483–2493, Sep. 2017.
37 *IEC 61850-5 2013: Communication networks and systems for power utility automation*, International Electrotechnical Commission Std., 2013.
38 "IEEE standard for synchrophasor data transfer for power systems," *IEEE Std C37.118.2-2011 (Revision of IEEE Std C37.118-2005)*, pp. 1–53, Dec. 2011.
39 P. Kansal and A. Bose, "Bandwidth and latency requirements for smart transmission grid applications," *IEEE Trans. Smart Grid*, vol. 3, no. 3, pp. 1344–1352, Sep. 2012.